ELSEVIER

Journal of Power Sources 81–82 (1999) 248–254

JOURNAL OF POWER SOURCES

www.elsevier.com/locate/jpowsour

Lithium transport through $Li_{1+\delta}[Ti_{2-y}Li_y]O_4$ $(y = 0; 1/3)$ electrodes by analysing current transients upon large potential steps

Su-Il Pyun *, Sung-Woo Kim, Heon-Cheol Shin

Department of Materials Science and Engineering, Korea Advanced Institute of Science and Technology, 373-1 Kusong-Dong, Yusong-Gu, Taejon 305-701, South Korea

Abstract

Lithium transport through $Li_{1+\delta}[Ti_{2-y}Li_y]O_4$ ($y = 0$; $1/3$) electrodes in the coexistence of a Li-poor phase α and a Li-rich phase β was investigated during electrochemical lithium intercalation by using the potentiostatic current transient technique under large potential stepping. For this purpose, the galvanostatic charge–discharge curve and the cathodic current transient were obtained as functions of the lithium content $(1 + \delta)$ and the lithium injection potential, respectively. The charge–discharge curve showed a potential plateau due to the coexistence of two phases α and β. The values of the quasi-equilibrium potential and the corresponding stoichiometry of the α- and β-phases were determined from the potential plateau. A three-stage current transient was observed as the applied potential step went below the potential plateau, and the second stage of this current was found to be governed by the diffusion-controlled phase boundary movement between the α- and β-phases.

Keywords: $Li_{1+\delta}[Ti_{2-y}Li_y]O_4$ electrode; Lithium transport; Diffusion-controlled phase boundary movement; Three-stage current transient; Large potential stepping

1. Introduction

Over the past decade, most studies on the electrochemical lithium intercalation into the transition metal oxides have been devoted to the diffusion of the lithium ion within a single-phase region, assuming that the diffusion is the rate-controlling process [1–3]. From the analysis of the three-stage current transients based on the concept of quasi-equilibrium [4], it has been recently reported that the lithium transport through the $LiCoO_2$ electrode proceeds by the diffusion-controlled phase boundary movement in the coexistence of two phases of a Li-poor phase α and a Li-rich phase β. This means that the potentiostatic current transients actually monitor the lithium transport involving the diffusion-controlled phase boundary movement through the electrode.

The spinel oxides $LiTi_2O_4$ and $Li[Ti_{5/3}Li_{1/3}]O_4$ are the end members of the solid solution series $Li[Ti_{2-y}Li_y]O_4$ for $0 \le y \le 1/3$ [5,6]. Although the two compounds, which are neighbouring phases in the ternary Li–Ti–O phase diagram, have the same crystal structure of cubic-spinel with a space group $Fd\bar{3}m$, they exhibit different thermodynamic characteristics such as electrode potential and stoichiometry [7,8]. Therefore, it is conceivable that the analysis of the current transient during the lithium intercalation gives us a better understanding of the lithium transport.

The present work discusses the lithium transport through $Li_{1+\delta}[Ti_{5/3}Li_{1/3}]O_4$ and $Li_{1+\delta}Ti_2O_4$ electrodes in the coexistence of two phases called α and β. For this purpose, the galvanostatic charge–discharge curve was obtained from both electrodes as a function of the lithium content $(1 + \delta)$. In addition, the cathodic current transient was measured as a function of lithium injection potential.

2. Experimental

$Li[Ti_{5/3}Li_{1/3}]O_4$ powder was prepared by heating a pressed mixture of TiO_2 (anatase) and $LiOH \cdot H_2O$ at 800°C for 24 h in air. The reaction product was ground for several hours by using an agate mortar and a pestle. $LiTi_2O_4$ powder was synthesized by chemically lithiating TiO_2 powder with 1.6 M *n*-butyllithium in hexane in a glove box (VAC HE403) for 1 week at ambient temperature [9]. The resulting product was filtered and washed with hexane and finally heated at 850°C for 24 h under

* Corresponding author. Tel.: +82-42-869-3319; Fax: +82-42-869-3310; E-mail: sipyun@sorak.kaist.ac.kr

0378-7753/99/$ - see front matter
PII: S0378-7753(99)00196-2

vacuum. To identify the crystal structures of the $Li[Ti_{5/3}Li_{1/3}]O_4$ and $LiTi_2O_4$ powders, X-ray diffraction patterns were recorded on an automated Rigaku powder diffractometer using Cu K_α radiation over the scanning angle 2θ range of 10° to 100° at the scan rate of 4°/min. The $Li[Ti_{2-y}Li_y]O_4$ ($y = 0$; 1/3) powders were mixed with 6 wt.% Vulcan XC-72 carbon black and 2 wt.% PVDF (polyvinylidenefluoride) in NMP (*N*-methylpyrrolidone). The stirred mixture was spread on 316 stainless steel ex-met. After evaporating the NMP, the carbon-dispersed composite electrode specimen was dried for 6 h under vacuum.

A three-electrode cell was employed for the electrochemical experiments. Both the reference and counter electrodes were lithium foils (Foote Mineral, USA, purity 99.9%). A 1 M $LiClO_4$ solution in propylene carbonate (PC) was used as the electrolyte. The apparent geometric area of the working electrode amounted to 2 cm^2.

The galvanostatic charge–discharge curve was recorded by an EG&G PAR Model 263A potentiostat/galvanostat under remote control of an IBM compatible personal computer. The current was selected in such a way the lithium content of $Li_{1+\delta}[Ti_{2-y}Li_y]O_4$ ($y = 0$; 1/3) would change by $\Delta\delta = 1$ after 5 h.

The potentiostatic current transient experiments were performed by applying various large potential steps (0.1 to 0.4 V). In the case of the $Li_{1+\delta}[Ti_{5/3}Li_{1/3}]O_4$ electrode, the cathodic current transient [1] was measured for 8×10^3 s when the initial potential of 1.7 $V_{Li/Li+}$ was dropped to lithium injection potentials between 1.6–1.4 $V_{Li/Li+}$, whereas in the case of the $Li_{1+\delta}Ti_2O_4$ electrode, the initial potential of 1.6 $V_{Li/Li+}$ was dropped to lithium injection potentials between 1.5–1.2 $V_{Li/Li+}$. Prior to the lithium intercalation, both electrodes were held at the initial potential for 2×10^3 s to obtain a low, steady-state current. All of the electrochemical experiments were conducted at ambient temperature in a glove box (MECAPLEX GB94) filled with purified argon gas.

3. Results and discussion

3.1. XRD characterization for the synthesized $Li[Ti_{5/3}Li_{1/3}]O_4$ and $LiTi_2O_4$ powders

Fig. 1(a) and (b) present X-ray diffraction pattern of the $Li[Ti_{5/3}Li_{1/3}]O_4$ and $LiTi_2O_4$ powders, respectively. By assuming the structure to be a cubic-spinel, all diffraction peaks can be indexed to determine the lattice parameter $a = 8.373$ Å for $Li[Ti_{5/3}Li_{1/3}]O_4$ and $a = 8.404$ Å for $LiTi_2O_4$. These values were in good agreement with those obtained by Harrison et al. [6]. From the XRD patterns,

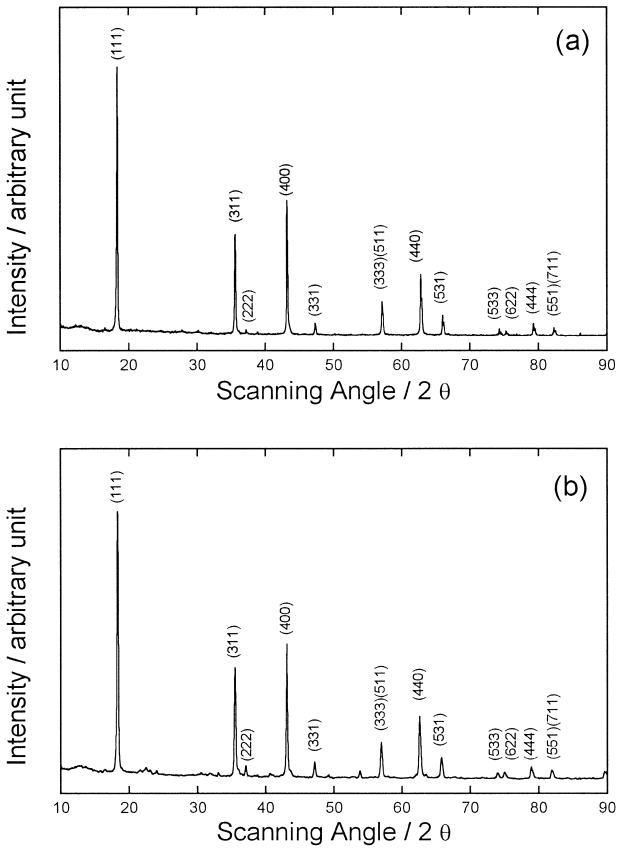

Fig. 1. X-ray diffraction patterns of (a) the $Li_{1+\delta}[Ti_{5/3}Li_{1/3}]O_4$ powder obtained by heating a mixture of TiO_2 and $LiOH \cdot H_2O$ at 800°C for 24 h in air and (b) the $Li_{1+\delta}Ti_2O_4$ powder obtained by heating a lithiated TiO_2 at 800°C for 24 h under vacuum. The Miller indices of the Bragg peaks are indicated over the each peak.

both oxides were clearly identified as being composed of a single-phase spinel with a space group $Fd\bar{3}m$.

3.2. Analysis of the galvanostatic charge–discharge curves of the $Li_{1+\delta}[Ti_{5/3}Li_{1/3}]O_4$ and $Li_{1+\delta}Ti_2O_4$ electrodes

Fig. 2(a) and (b) give the second galvanostatic charge-discharge curve obtained from the $Li_{1+\delta}[Ti_{5/3}Li_{1/3}]O_4$ and $Li_{1+\delta}Ti_2O_4$ electrodes, respectively, as a function of lithium content $(1 + \delta)$. The deviation δ from the ideal stoichiometry ($\delta = 0$) was calculated from the mass of the oxide and the electric charge that was transferred during the electrochemical lithium intercalation and deintercalation. In the present work, the galvanostatic charge–discharge curve and potentiostatic current transient were measured on the electrode which previously underwent one cycle of charge–discharge in order to eliminate the effect of the initial irreversible capacity on both charge–discharge curve and current transient.

The charge–discharge curve for the $Li_{1+\delta}[Ti_{5/3}Li_{1/3}]O_4$ and $Li_{1+\delta}Ti_2O_4$ electrodes showed a potential plateau near 1.56 $V_{Li/Li+}$ and 1.38 $V_{Li/Li+}$, respectively. The occurrence of these plateaus is due to the coexistence

[1] This is measured during the lithium intercalation and sometimes termed build-up current transient in the literature.

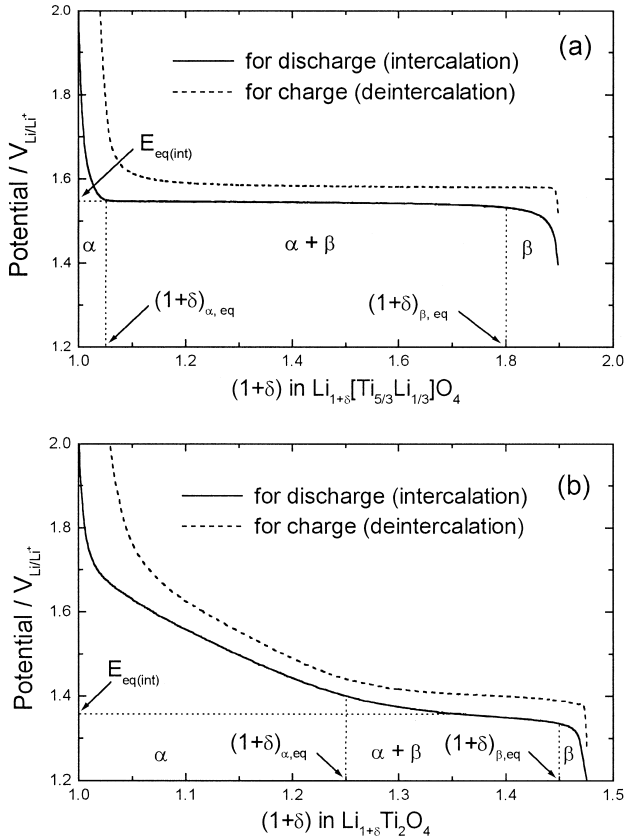

Fig. 2. Second galvanostatic charge–discharge curves measured from the cell of Li/1 M $LiClO_4$-PC solution/(a) $Li_{1+\delta}[Ti_{5/3}Li_{1/3}]O_4$ and (b) $Li_{1+\delta}Ti_2O_4$. The change in lithium content, $\Delta\delta = 1$, for $Li_{1+\delta}[Ti_{2y}Li_y]O_4$ occurs over 5 h.

of two phases of a Li-poor phase α and a Li-rich phase β [10]. Comparing the charge–discharge curve for the $Li_{1+\delta}[Ti_{5/3}Li_{1/3}]O_4$ electrode with that curve for the $Li_{1+\delta}Ti_2O_4$ electrode, the width of the stable α-phase region of the former electrode is much narrower than that of the latter electrode. From the fact that both electrodes have the same crystal structure, the difference in the shape of the charge–discharge curve can be mainly derived from the difference in the value of the effective interaction energy between lithium ions due to the difference in the chemical composition of the electrodes. According to a lattice-gas model with interaction between the intercalated lithium ions, phase separation occurs for the effective attraction between the lithium ions [11]. Since lithium ion moves zigzag through the three-dimensional network of 8(a) and 16(c) sites during the intercalation, the effective interaction energy between the lithium ions in the $Li_{1+\delta}[Ti_{5/3}Li_{1/3}]O_4$ electrode is greater than in the $Li_{1+\delta}Ti_2O_4$ electrode by the additional attractive interaction with the lithium ion located at 16(d) site in the former electrode. This means that the formation of the β-phase in the former electrode already occurs at a lower lithium concentration $(1+\delta)$ as compared to the latter electrode.

In the previous work [4,12], it was suggested that the lithium transport through the $LiCoO_2$ electrode involves a diffusion-controlled phase boundary movement in the co-existence of two phases α and β. Based on this concept of quasi-equilibrium, the following approximated values for the $Li_{1+\delta}[Ti_{5/3}Li_{1/3}]O_4$ electrode can be obtained from Fig. 2(a): the quasi-equilibrium potential during the lithium intercalation $E_{eq(int)}$ was 1.55 $V_{Li/Li+}$ and the quasi-equilibrium stoichiometries at the α/β phase boundary for the α-phase side $(1+\delta)_{\alpha,eq}$ and for the β-phase side $(1+\delta)_{\beta,eq}$ were 1.05 and 1.8, respectively. For the $Li_{1+\delta}Ti_2O_4$ electrode, the values are estimated from Fig. 1(b) in the same way: $E_{eq(int)} = 1.36$ $V_{Li/Li+}$, $(1+\delta)_{\alpha,eq} = 1.25$ and $(1+\delta)_{\beta,eq} = 1.45$. These values were used for the analysis of the potentiostatic current transients.

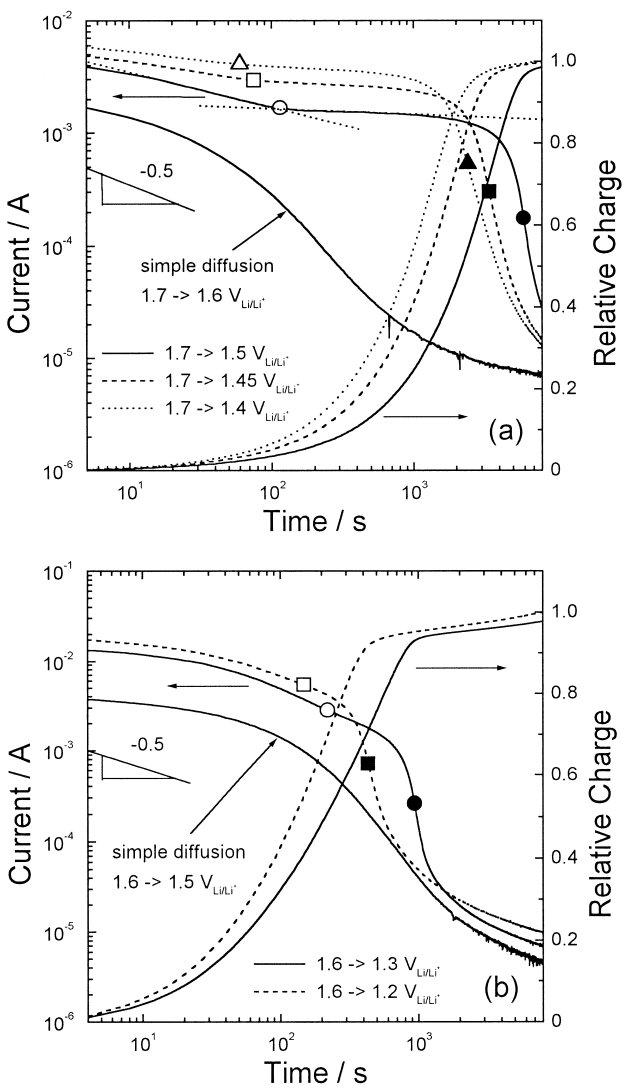

Fig. 3. Typical cathodic current transients and corresponding relative charge transients obtained from (a) the $Li_{1+\delta}[Ti_{5/3}Li_{1/3}]O_4$ electrode and (b) the $Li_{1+\delta}Ti_2O_4$ electrode in 1 M $LiClO_4$–PC solution at various lithium injection potentials as indicated in the figures. The open symbols (○, □, △) and the closed symbols (●, ■, ▲) represent the first to the second stage transition times (t_{T1}) and the second to the third stage transition times (t_{T2}), respectively.

3.3. Analysis of the cathodic current and relative charge transients for the $Li_{1+\delta}[Ti_{5/3}Li_{1/3}]O_4$ and $Li_{1+\delta}Ti_2O_4$ electrodes

Fig. 3(a) and (b) present the cathodic current transients on a logarithmic scale with the corresponding relative charge transients on a semi-logarithmic scale which were obtained from the $Li_{1+\delta}[Ti_{5/3}Li_{1/3}]O_4$ and $Li_{1+\delta}Ti_2O_4$ electrodes in 1 M $LiClO_4$–PC solution at various lithium injection potentials as indicated in the figures. The relative charge is defined as the measured charge divided by the maximum charge transferred reversibly during the lithium intercalation.

From the concept of quasi-equilibrium, it was expected that the lithium content of the $Li_{1+\delta}[Ti_{5/3}Li_{1/3}]O_4$ electrode would change within the region of the α-phase as the initial potential of 1.7 $V_{Li/Li+}$ was dropped to a lithium injection potential of 1.6 $V_{Li/Li+}$. The two-stage current transient obtained in this case (Fig. 3(a)) suggests that the lithium intercalation into the $Li_{1+\delta}[Ti_{5/3}Li_{1/3}]O_4$ electrode proceeded by a simple finite-length diffusion within the α-phase. It is well known that for such a diffusion, the current transient exhibits a linear relationship with a constant slope followed by a steep exponential decay where, under potentiostatic conditions, the slope in the initial stage must be $-1/2$ on a logarithmic scale [13,14]. However, the slope in the first stage in Fig. 3(a) and (b) was flatter than $-1/2$. This indicates that the lithium transport in the $Li_{1+\delta}[Ti_{5/3}Li_{1/3}]O_4$ and $Li_{1+\delta}Ti_2O_4$ electrodes is controlled not only by the simple finite-length diffusion but also by another process. In the previous work on $Li_{1-\delta}CoO_2$ [15], it was suggested that only a small fraction of the surface area of the composite electrode in contact with the electrolyte provides active sites necessary for the lithium intercalation and that the active surface area of the composite electrode that is in contact with the electrolyte varies with the lithium content. Therefore, the deviation of the slope in the first stage from $-1/2$ could be attributed to the particulated geometry of the composite electrode [1].

A three-stage behaviour was observed in the current transient for the $Li_{1+\delta}[Ti_{5/3}Li_{1/3}]O_4$ electrode as the initial potential of 1.7 $V_{Li/Li+}$ was dropped to a lithium injection potential that was lower than the quasi-equilibrium potential of 1.55 $V_{Li/Li+}$. The first transition time t_{TI} (Fig. 3(a)) is determined as the very time at which the tangent line of the first stage curve intersects that of the second stage curve [16]. The second transition time t_{T2} (Fig. 3(a)) separating the second and the third stage of the lithium transport is characterized as the time at the inflection point of the current transient for which $((d^2 \log I)/(d(\log t)^2)) = 0$ [4,12]. The first stage $(0 \le t < t_{T1})$ of the three-stage current transient in Fig. 3(a) resembled the initial stage of the two-stage current transient where the potential was dropped from 1.7 to 1.6 $V_{Li/Li+}$. On the other hand, in the second stage $(t_{T1} < t < t_{T2})$ the three-stage current transient deviated remarkably from the two-stage one. As the potential step increased, the current in the second stage increased and the transition times t_{T1} and t_{T2} were reached sooner.

The relative charge transient for the $Li_{1+\delta}[Ti_{5/3}Li_{1/3}]O_4$ electrode shown in Fig. 3(a) increased almost linearly with lithium injection time during the second stage. The relative charge transferred during $0 \le t < t_{T1}$, however, corresponded to the range of the quasi-equilibrium stoichiometry of the α-phase whereas the relative charge transferred during $t_{T1} < t < t_{T2}$ was used to increase the fraction of the β-phase in the coexistence region of α and β (cf. Fig. 2(a)).

In Fig. 3(b), the cathodic current transients and the corresponding relative charge transients for the $Li_{1+\delta}Ti_2O_4$ electrode at various lithium injection potentials showed

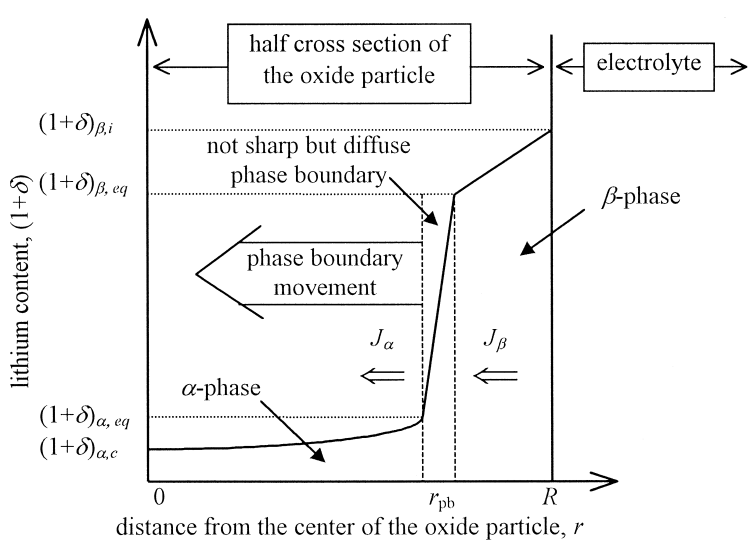

Fig. 4. Schematic diagram of the lithium content profile for the moving phase boundary during the electrochemical lithium intercalation.

features similar to those of the $Li_{1+\delta}[Ti_{5/3}Li_{1/3}]O_4$ electrode, except that the first stage of the three-stage current transients of the former electrode are more prolonged than those of the latter electrode. This is consistent with the result obtained from the galvanostatic charge–discharge curve where the width of the stable α-phase region of $Li_{1+\delta}Ti_2O_4$ is broader than that of $Li_{1+\delta}[Ti_{5/3}Li_{1/3}]O_4$.

Analysing the three-stage current transient, Choi et al. [4] suggested a schematic diagram for the moving phase boundary during the electrochemical lithium intercalation as shown in Fig. 4. R is the radius of the oxide particle, r represents the distance from the center of the oxide particle, r_{pb} marks the distance from the center of the oxide particle to the α/β phase boundary, $(1+\delta)_{\beta,i}$ denotes the stoichiometry at the interface between the surface of the oxide particle and the electrolyte, $(1+\delta)_{\alpha,c}$ indicates the stoichiometry at the center of oxide particle and $(1+\delta)_{\alpha,eq}$ and $(1+\delta)_{\beta,eq}$ represent the quasi-equilibrium stoichiometries at the α/β phase boundary.

The lithium ion diffuses from the surface of the spinel $Li_{1+\delta}[Ti_{2-y}Li_y]O_4$ ($y=0$; $1/3$) particle zigzag through the three-dimensional network of the tetrahedral 8(a) and octahedral 16(c) sites towards the center of the oxide particle [17,18]. For the analysis of the diffusing fluxes inside the $Li_{1+\delta}[Ti_{5/3}Li_{1/3}]O_4$ and $Li_{1+\delta}Ti_2O_4$ electrodes, we must therefore take the spherical symmetry of these particles into account. According to Fick's first law, the flux $J_\beta = -\tilde{D}_{Li^+,\beta}[(\partial(1+\delta))/(\partial r)]_\beta$ $(r_{pb} < r < R)$ flows from the surface of the oxide particle towards the α/β phase boundary and the flux $J_\alpha = -\tilde{D}_{Li^+,\alpha}[(\partial(1+\delta))/(\partial r)]_\alpha$ $(0 < r < r_{pb})$ flows from the α/β phase boundary towards the center of the oxide particle during the lithium intercalation.

Dropping the applied potential from E_1 to E_2 created a concentration difference of $[(1+\delta)_{\beta,i} - (1+\delta)_{\alpha,c}]$ between the surface and the center of the oxide particle. Thus, the potential step $(E_1 - E_2)$, which caused that concentration gradient, acted as the driving force for the diffusion of the lithium ion. The experimental findings above showed that the relative charge transferred during $0 \le t < t_{T1}$ is approximately equal to the relative charge needed for the α-phase to reach its quasi-equilibrium stoichiometry of $(1+\delta)_{\alpha,eq}$ in $Li_{1+\delta}[Ti_{5/3}Li_{1/3}]O_4$ or $Li_{1+\delta}Ti_2O_4$. This indicates that the lithium transport through both electrodes was mainly controlled by a simple finite-length diffusion of the lithium ion within the α-phase which made up the particle interior.

Once the stoichiometric limit $(1+\delta)_{\alpha,eq}$ of the α-phase was reached, the α/β phase boundary moved towards the center of the oxide particle as long as $J_\beta > J_\alpha$, which was caused by $(E_{eq(int)} - E_2) > 0$. Because the lithium ion diffusion was determined by the concentration gradient $[(\partial(1+\delta))/(\partial r)]_\beta$ across the outer β-phase, the driving force for the phase boundary movement decreased gradually as the phase boundary moved towards the center of the oxide particle. This model of the phase boundary movement is supported by Fig. 3 where the current in the second stage was proportional to the driving force $(E_{eq(int)} - E_2)$ while decreasing remarkably slower than in the two-stage process that represented a simple finite-length diffusion.

Finally, when the α/β phase boundary reached the center of the oxide particle, the movement of phase boundary came to an end and caused the lithium ions to undergo a simple finite-length diffusion within the β-phase. This scenario occurred during the third stage of the current transient where the lithium transport was used for increasing the lithium concentration $(1+\delta)_\beta$ of the β-phase beyond $(1+\delta)_{\beta,eq}$.

Fig. 5(a) and (b) illustrate the derivatives of the logarithmic current transients from Fig. 3(a) for the $Li_{1+\delta}[Ti_{5/3}Li_{1/3}]O_4$ electrode and from Fig. 3(b) for the

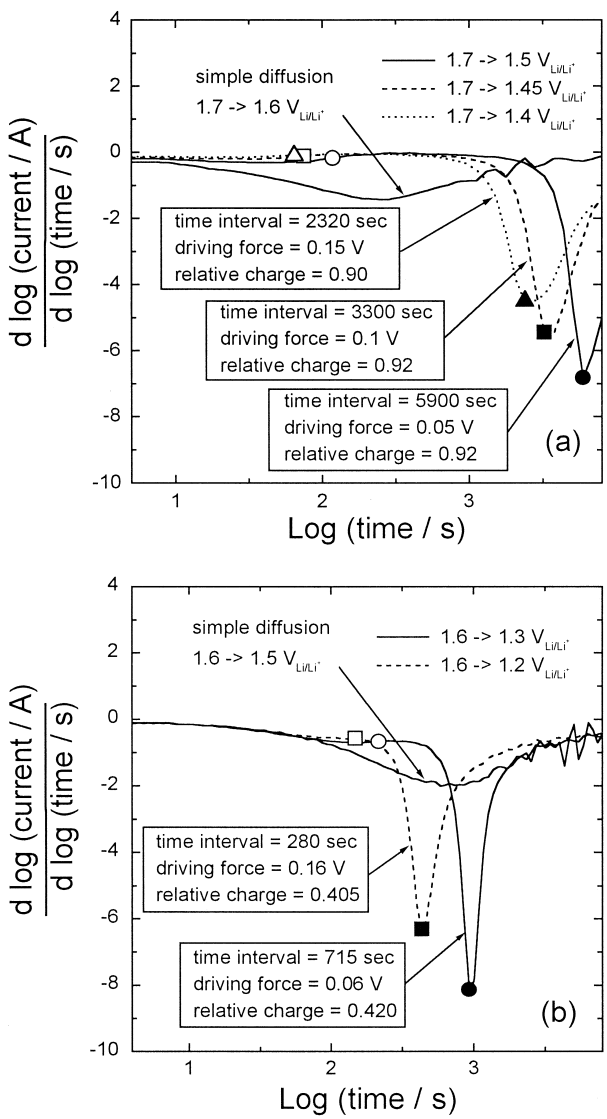

Fig. 5. Derivatives of logarithmic current transients obtained from (a) the $Li_{1+\delta}[Ti_{5/3}Li_{1/3}]O_4$ electrode and (b) the $Li_{1+\delta}Ti_2O_4$ electrode in 1 M $LiClO_4$–PC solution at various lithium injection potentials as indicated in the figures. The time interval between t_{T1} (open symbol) and t_{T2} (closed symbol), the driving force $(E_{eq(int)} - E_2)$ and the relative charge are indicated in the figures.

$Li_{1+\delta}Ti_2O_4$ electrode, respectively, with respect to the logarithmic time at various lithium injection potentials as indicated in figures. The time interval between the first transition time t_{T1} and the second transition time t_{T2}, the driving force for the phase boundary movement and the relative charge transferred during the second stage of each transient are indicated in the figures.

In view of the fact that the lithium transport mainly proceeded by the diffusion-controlled phase boundary movement in the second stage, it is not surprising that the time interval for lithium injection in Fig. 5(a) and (b) was inversely proportional to the driving force $(E_{eq(int)} - E_2)$ of the phase boundary movement where the relative charge transferred during the phase boundary movement remained virtually constant and was therefore independent of the driving force. Evidently, this driving force did not only affect the time interval $(t_{T2} - t_{T1})$, but, as discussed above, proportionally determined the current transient during that lithium injection time. In order to eliminate the influence of the driving force from the curves shown in Fig. 3(a) and (b), we normalised the current and the time to the driving force. This was achieved by division and multiplication, respectively.

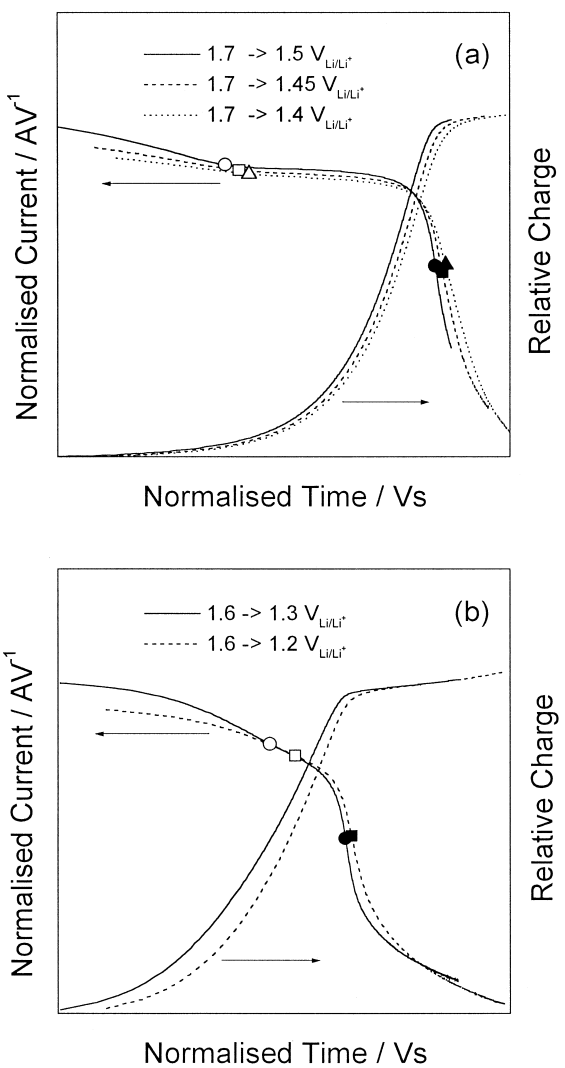

Fig. 6. Normalised current transients on a logarithmic scale with the corresponding relative charge transients on a semi-logarithmic scale obtained from (a) the $Li_{1+\delta}[Ti_{5/3}Li_{1/3}]O_4$ electrode and (b) the $Li_{1+\delta}Ti_2O_4$ electrode at various lithium injection potentials as indicated in the figures. The open symbols and the closed symbols represent the first to the second stage transition times (t_{T1}) and the second to the third stage transition times (t_{T2}), respectively.

Fig. 6(a) and (b) illustrate the resulting normalised current transients on a logarithmic scale with the corresponding relative charge transients on a semilogarithmic scale obtained from the $Li_{1+\delta}[Ti_{5/3}Li_{1/3}]O_4$ and $Li_{1+\delta}Ti_2O_4$ electrodes at various lithium injection potentials as indicated in the figures. The normalised current transients and the relative charge transients of the second stage now coincide with each other. This confirms that the lithium transport through the $Li_{1+\delta}[Ti_{2-y}Li_y]O_4$ $(y = 0;\ 1/3)$ electrodes in the coexistence of the two phases α and β is mainly governed by the diffusion-controlled phase boundary movement. However, the first and the third stage of the normalised current transients do not coincide, since the lithium transport in those stages is barely governed by the diffusion-controlled phase boundary movement. The analysis of the three-stage current transients above demonstrated that the concept of quasi-equilibrium could satisfactorily be applied to the lithium transport through $Li_{1+\delta}[Ti_{2-y}Li_y]O_4$ $(y = 0;\ 1/3)$ electrodes involving a diffusion-controlled phase boundary movement.

4. Conclusions

The present work considers lithium transport through $Li_{1+\delta}[Ti_{5/3}Li_{1/3}]O_4$ and $Li_{1+\delta}Ti_2O_4$ electrodes in the coexistence of two phases α and β on the basis of the concept of quasi-equilibrium. From the experimental results, the following conclusions are drawn.

(1) The occurrence of a potential plateau in the charge–discharge curve was due to the coexistence of two phases of a Li-poor phase α and a Li-rich phase β. Based upon the concept that the α- and β-phases were in quasi-equilibrium with each other in the region of the potential plateau, the quasi-equilibrium potential and the corresponding quasi-equilibrium stoichiometry of each phase could be determined.

(2) The typical cathodic current transient which was obtained from both electrodes in the coexistence of two phases consisted of three stages. When normalising the current and the time to the driving force $(E_{eq(int)} - E_2)$ of the phase boundary movement, the current transients of the second stage coincided with each other. This suggests that the lithium transport through both electrodes in the coexistence of the two phases α and β proceeded mainly by the diffusion-controlled phase boundary movement.

Acknowledgements

The receipt of research grant under the programme 'Development of technology of high performance batteries for electric vehicle application 1997/1998' from the Ministry of Commerce and Industry, Korea is gratefully acknowledged. Incidentally, this work was supported in the period of 1997/1998 by the Korea Science and Engineering Foundation (KOSEF) through the Center for Interface Science and Engineering of Materials at Korea Advanced Institute of Science and Technology (KAIST).

References

[1] A.J. Vaccaro, T. Palanisamy, R.L. Kerr, J.T. Maloy, J. Electrochem. Soc. 129 (1982) 682–688.
[2] S. Bach, J.P. Pereira-Ramos, N. Baffier, R. Messina, J. Electrochem. Soc. 137 (1987) 1042–1047.
[3] N. Kumagai, I. Ishiyama, K. Tanno, J. Power Sources 20 (1987) 193–198.
[4] Y.-M. Choi, S.-I. Pyun, J.M. Paulsen, Electrochim. Acta 44 (1998) 623–632.
[5] A. Deschanvres, B. Raveau, Z. Sekkal, Mater. Res. Bull. 6 (1971) 699–704.
[6] M.R. Harrison, P.P. Edwards, J.B. Goodenough, Philos. Mag. B 52 (1985) 679–699.
[7] K.M. Colbow, J.R. Dahn, R.R. Haering, J. Power Sources 26 (1989) 397–402.
[8] K. West, B. Zachau-Christiansen, T. Jacobsen, S. Skaarup, Mater. Res. Soc. Symp. Proc. 293 (1993) 39–47.
[9] M.S. Whittingham, M.B. Dines, J. Electrochem. Soc. 124 (1977) 1387–1388.
[10] M.B. Armand, in: D.W. Murphy, J. Broadhead, B.C.H. Steele (Eds.), Materials for Advanced Batteries, Plenum, New York, 1980, pp. 145–161.
[11] W.R. McKinnon, R.R. Haering, in: R.E. White, J.O'M. Bockris, B.E. Conway (Eds.), Modern Aspects of Electrochemistry, Vol. 15, Plenum, New York, 1983, pp. 235–304.
[12] H.-C. Shin, S.-I. Pyun, Electrochim. Acta 44 (1999) 2235–2244.
[13] C.J. Wen, B.A. Boukamp, R.A. Huggins, W. Weppner, J. Electrochem. Soc. 126 (1979) 2258–2266.
[14] J.-S. Bae, S.-I. Pyun, Solid State Ionics 90 (1996) 251–260.
[15] Y.-M. Choi, S.-I. Pyun, Solid State Ionics 109 (1998) 159–163.
[16] S.-I. Pyun, J.-N. Han, T.-H. Yang, J. Power Sources 65 (1997) 9–13.
[17] S.-I. Pyun, Y.-M. Choi, I.-D. Jeng, J. Power Sources 68 (1997) 593–599.
[18] D.W. Murphy, R.J. Cava, S.M. Zahurak, A. Santoro, Solid State Ionics 9–10 (1983) 413–418.